SCREW-IN SOIL NAIL FOR SLOPE REINFORCEMENT AGAINST SLIP FAILURE: A LAB-BASED MODEL STUDY

*Chee-Ming Chan[1] and Muhammad Halim Ab. Raman[2]

[1&2]Faculty of Engineering Technology, Universiti Tun Hussein Onn Malaysia, Malaysia

ABSTRACT: Slope failures occur when the shear resistance along the slip plane is exceeded. This can be caused by excessive load imposed at the slope crest or compromised stability of the slope, e.g. disturbed dimensions of the slope. In order to prevent slope failure, stabilisation or reinforcement measures need to be taken. A common solution is to intercept the slope failure plane with reinforcement elements, such as soil nails and ground anchors. In soil nailing, reinforcement bars are installed on the slope to effectively resist the additional shear forces from the imposed loads, hence reducing the probability of failure in the long run. This paper describes the innovation of soil nail with screw-in installation mechanism instead of the conventional push-in approach. The screw-in installation ensures better soil-nail grip and less disturbance during the slope stabilisation procedure, especially in terms of noise and spoils. In addition, the novel nail has a hollow stem which improves shear resistance with greater soil-nail surface contact on the inner wall. The opening at the nail head also enables displaced air to escape as the nail is screwed into the slope and soil pushed into the inner hollow cavity. The prototype nails were tested in a slope model with different configurations, and were found to reduce the Angular Distortion Ratio by 37 % and the Volumetric Deformation Index as much as 33 % respectively. The novel screw-in soil nail could be potentially used to stabilize natural and man-made slopes, though full-scale simulations are recommended to formulate the installation procedure and to validate the effectiveness.

Keywords: slope failure, soil nail, friction, slip plane, load-bearing, displacement, shearbox test

1. INTRODUCTION

Slopefailures are major natural hazards in many areas around the world. Slopes fail due to a variety of reasons, including self-load, water influx, erosion and undercutting of slopes for construction. In addition, the constant gravity force pulls the slope downward and outward slowlywith time, inadvertently affecting the condition of structures constructed on top of it [1].

Groundwater table fluctuation is one of the key factors leading to slope failures, especially in regions with seasonal, excessive rainfalls. Groundwater consists largely of surface runoff that seeps into the ground, a hydrological result of infiltration of rain water on the permeable slope surface. Rain water that runs off a slope can cause surface erosion in the absence of adequate surface protection too. High permeability soil infiltrates majority of runoff water into the subsoil, consequently raising the groundwater level in the slope and affects the effective shear resistance of the soil against slippage.Besides, seepage adds weight to the slope by replacing air in the soil pores. The increased self-weight of the saturated soil would create additional stresses which can lead to slope instability. Some examples of past work on the rain water seepage on slope stability have been reported by Cai&Ugai [2], Dahal et al. [3], Deepa & Viswanadham [4], Guan et al. [5] as well as Raj & Sengupta [6].

Weathering of slope surface is an integral part of any grounds, and the process may proceed rapidly over time if no preventive action is taken. Weathering would first dislodge the materials on the surface and proceed to loosen the soil particle bondage below the surface. The process further endangers the slope by introducing infiltration pathways into deeper zones of the slope, compromising the soil's shear strength and eventually leading to failures. In addition, external loads, such as building foundations, applied at slope crest could increase the overall gravitational force acting on the slope beyond its resistance. This includes temporary dumping of spoil during construction stage near a slope crest, where the overloading effect could lead to severe slope failure.

The need for infrastructure development exerts an immense demand for both engineered cut and fill slopes to provide for the growing population and nation building as a whole. Slopes, whether manmade or natural, once disturbed for construction, must be carefully analysed in terms of short and long term stability. Slope safety investigations are often accompanied by numerical computations and simulations, which results are used to formulate suitable, effective stabilization methods. Slope stabilization methods often involve specialty construction techniques that must be

fully understood and modeled out in realistic ways [7].

Malaysia has experienced a number of slope failure cases in recent years, involving the loss of lives and damages of property and other infrastructure (Fig. 1). In August 2011, the slope failure in Cameron Highlands killed 7 people seriously injured 2. In May the same year, the slope failure at Hulu Langat destroyed Madrasah At-Taqwa and killed 16 people [8]. Heavy rain and poor slope management overloading the drainage system was found to be the main trigger of the failure. In 2014, a morning heavy rainfall triggered significant movement in the slope backing some apartment blocks at Bukit Beruntung, leading to the evacuation of over 2000 residents. It was reported that the poorly designed cut slope was the main cause of the failure.
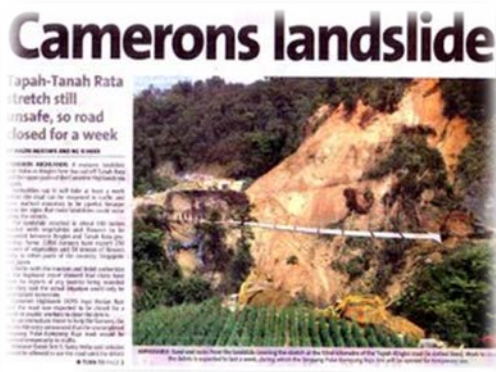
Cameron Highlands; 7 dead (NST, 2011).

Hulu Langat; 16 dead (BBC News, 2011).

Bukit Beruntung; 2000 evacuated (The Star, 2014).

Fig. 1 Slope failure tragedies in Malaysia.

It would appear that recurring slope failures is a devastating disaster in this country. Among the triggering factors are erosion, geomorphological processes including geological movement, erosion and deposition. Also, landscape instability was found to occur in conjunction with gully erosion presence [9]. This has led many experts to postulate the close correlation between rainfall intensity and soil strength on a slope in the prediction of failures.

Some popular slope stabilization methods include gabion wall, concrete retaining wall, vegetation covered slopes, placement of recycled tires, geoweb installation and micro pile stabilization. Soil nailing is perhaps one of the most economical and cost- as well as time-efficient techniques available though. It is used as a failure preventive measure for both unstable natural and engineered slopes. It is also used to restore stability to slopes showing signs of excess movements. The soil nailing technique involves the insertion of reinforcing bars into the slope, which effectively serves as structural element for load transfer to the ground [10].

A typical soil nail is shown in Fig. 2. The conventional soil nails can be divided into several types, primarily depending on the nail installation method. These include the following:

a. Driven nail: Mechanically pushed into the ground; quick installation but lacks long term corrosion protection; mostly for temporary works.
b. Launched nail: 'Shot' into the ground with compressed air; very quick installation but lacks penetration depth control.
c. Grouted nail: Drilling of cavity is followed by placement of nails; grout is then used to fill up the hole.
d. Self-drilling nail: Simultaneous driving of hollow bars and injection of grout; quicker than grouted nail installation with better corrosion protection.
e. Jet-grouted nail: High pressure grouting displaces soil to form cavity for nail placement; good corrosion protection.
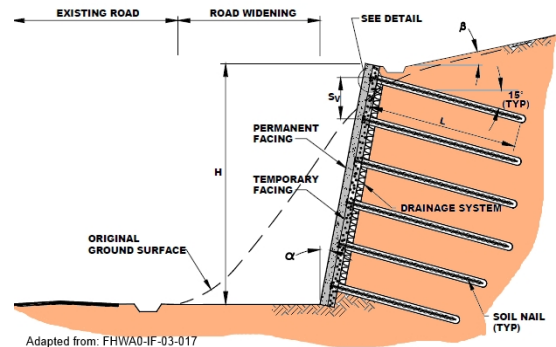
Fig. 2 Typical soil nail (china-steelpiling.com) [11].

The design of soil nailing can be found in FHWA ManualFHWA-NHI-14-007 (2015) "Geotechnical Engineering Circular No. 7: Soil Nail Walls" [12], BS8006-2: 2011 "Code of Practice for Strengthened / Reinforced Soils- Part 2: Soil Nail Design" [13], and BS EN 14490: 2010 "Execution of Special Geotechnical Works: Soil Nailing" [14]. Nonetheless individual companies usually have their own uniquely featured soil nails and installation procedure, adapted to the standards requirements. The design and analysis of soil nailing encompass 2 limiting conditions, namely strength and service limit states, as well as other design considerations [15]. Under the strength limit state analysis, consideration is made for external sliding, bearing capacity and global failure modes, and the internal nail-soil and bar-grout pullout failures, nail tensile as well as bending and shear failures. In addition, facing failures associated with flexure, punching shear and head-stud s are taken into account in the limit state analysis. On the other hand, the service limit state analysis calls for only the excessive wall deformation check. Other design considerations involve standard components of a soil nail installation, i.e. drainage behind the wall, corrosion and frost protection of nails, and the support of dead load from temporary facing.

Prashant& Mukherjee [10] compiled the pros and cons of soil nail installation. Some factors that make soil nailing preferable compared to other slope stabilization techniques are the simple and compact installation equipment, minimal traffic disruption with less congested work site, relatively quick installation process, flexibility of placement and installation, cost-effective in most cases, and better earthquake resistance due to the nails' pliability against deformation. However there are several disadvantages to the technique, such as unsuitability for grounds with high water table and granular soil formations, grounds with existing utilities like buried water pipes, corrosion of soil nail and the fundamental need of soil deformation to mobilize shear resistance, which is unacceptable in cases of stringent deformation requirements.

All in all soil nailing is a versatile, economical and highly adaptable slope stabilization technique. Past research work to refine the technique can be found in a number of publications. These reported works include the popular pullout test for soil nails, as conducted by McDonald & Ims [16], Su et al. [17] and Pei et al. [18]. In addition, Wang & Richwien [19] examined the soil-nail interface friction, while Yin et al. [20] investigated the effect of grouting pressure on the pullout resistance of a manmade compacted decomposed granite fill. Also, Yin &

Xu [21] reported on the expedience of installing soil nail for supporting a foundation pit. Besides, comparative work between soil nail and mechanical slope stabilization methods can be found in Turner & Jensen [22]. Numerical simulations and computational refinement of slope stabilization analysis were also reported, as exemplified in works by Li [23], Dahal et al. [3] and Farshidfar & Nayeri [24]. Nevertheless less effort seems to be directed at improving the nail installation process, especially for treating shallow slope failures as commonly encountered in Malaysia. This paper describes the novel innovation of a screw-in soil nail for minimal energy consumption, spoil production and noise disturbance during installation, while creating an effective soil-nail interface for long term slope safety. Scaled down prototype screw-in soil nails were designed and 3D-printed for simulations in an instrumented model setup.

2. MATERIALS AND METHODS

2.1 Simulated soil: SKW mixture
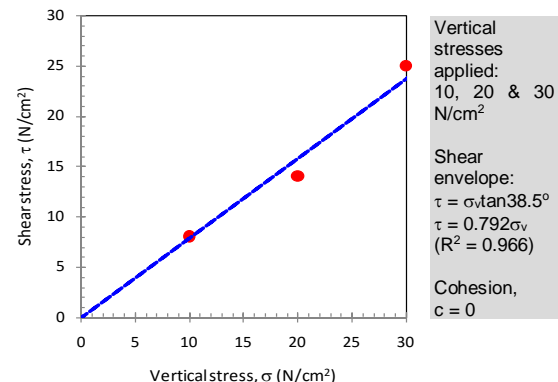
Fig. 3 Shear failure envelope for SKW.

To simulate the soil in the model, a mixture of sand, kaolin and water was prepared at the ratio of 8:2:1. Generally, kaolin or china clay is a clay mineral nearly white in color and with clay size particles (i.e. $< 2\mu m$) in the geotechnical categoristion. The sand used was classified as a poorly graded sand with more than 50 % portion passing the 425 μm sieve. The rather uniform sand was adopted in the mixture to (1) lend texture to the simulated soil, and to (2) enhance the soil-nail frictional resistance in the model test. A conventional kitchen mixer was used for mixing, where dry kaolin powder was first hand-mixed with sand before water was added for mechanical mixing. For simplicity, the sand-kaolin-water mixture was named SKW.

The mixture was next tested in the shearbox (6 cm x 6 cm x 12 cm) to determine the undrained shear strength parameters. Vertical stresses (σ) of 10, 20 and 30 N/cm^2 were applied to obtain the

corresponding maximum shear stresses (τ) mobilized. From the τ-σ plot in Fig. 3, the shear failure envelope was derived and defined by the equation $\tau = 0.792\sigma$, which gives the frictional angle (ϕ) of the SKW mixture as 38.5º, or $\tau = \sigma\tan38.5º$ (Fig. 3). Note that despite the presence of 20 % kaolin in the SKW mixture, sand dominated the shear strength mobilization by frictional resistance, where cohesion (c) was found to be zero (y-axis interception of the τ-σ plot). The SKW produced the optimum workability for compaction in the model box to form the slope.

2.2 Screw-in soil nail: Prototype design
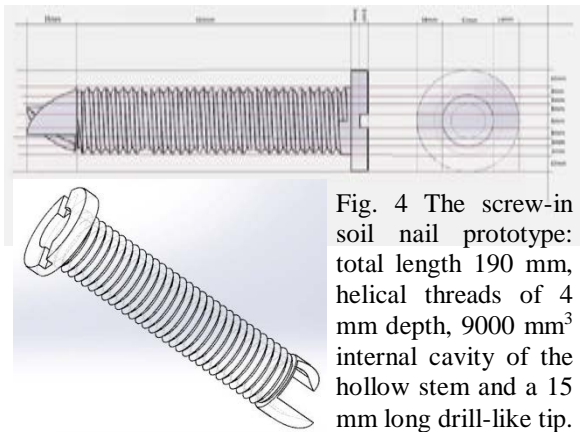
Fig. 4 The screw-in soil nail prototype: total length 190 mm, helical threads of 4 mm depth, 9000 mm³ internal cavity of the hollow stem and a 15 mm long drill-like tip.

Design of the soil nail revolved around the key concern of ease of installation with minimal disturbance to the surrounding soil. The screw-in mechanism enables a smooth nail installation process. On a scale of 1:10, the soil nail prototype was 3D printed using a fused deposition modeling machine. The prototype nail measured 190 mm in length, with the 4 mm deep threaded stem covering 165 mm of the total length (Fig. 4). The threads followed a helical spiral at a slight slanting angle ($\approx$10º to the horizontal plane). The threaded surface also provided grater contact surface with the ground when installed, resulting in better frictional grip and pullout resistance. The nail's stem was hollow with an inner diameter of 24 mm within a 4 mm thick wall. This gave the hollow stem a 9000 mm³ internal volume. The outer 4 mm thickness formed the helical thread spiral mentioned earlier. The stem was capped by a 60 mm diameter circular nail head of 10 mm thickness. A 5 mm deep groove was formed across the top of the nail head for insertion of the straight head manual driving tool. During installation, the displaced soil would be pushed into the cavity in the stem to provide increased contact surface for frictional resistance. This was intended as substitution to the grouting method which is in general more disruptive with spoils production. With a 15 mm long pointed tip shaped like a drill

bit, no pre-drilled holes or boring procedure was necessary in the installation of this screw-in soil nail, where a rotating mechanism of the nail head was sufficient to initiate the driving process.

2.3 Setup of model box
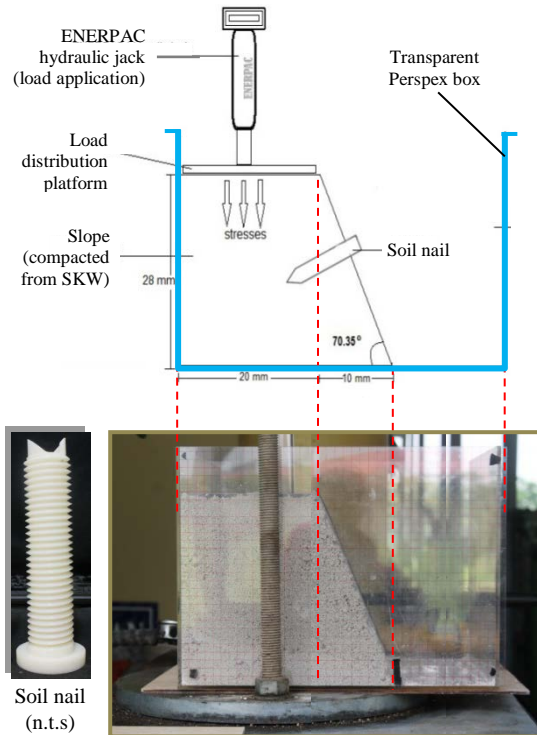
Fig. 5 Model box setup for simulation of slope reinforced with the screw-in soil nail(s).

Measuring 400mm x 300mm x 300mm, the model box was constructed using Perspex to produce a see-through observation chamber (Fig. 5). Gridlines were drawn on the front facing of the box for measurements of the slope deformation post-test. The slope was erected by light compaction of the SKW in layers to the final dimensions of 28 mm height, 30 mm base width with a 70.35º gradient to the horizontal plane. A platform was placed at the slope crest (20 mm width) to ensure uniform distribution of the load applied. Compressive load was introduced via the ENERPAC hydraulic jack system, where a piston touching the platform transferred the load onto the slope. The vertical stress applied was kept constant at 700 kPa throughout each test. The slope was considered to have failed and the test terminated when vertical deformation of the slope reached 56 mm, or equivalent to 20 % of the slope height. Note that as discussed in subsequent sections, the model slope showed corresponding shallow landslide type failure in all cases. A total of 5 test configurations were examined in the model tests, namely

1. C: control; unreinforced slope.

2. CN1: single control nail (smooth surface)
3. CN3: triple control nails (smooth surface)
4. IN1: single innovative nail (screw-in type)
5. IN3: triple innovative nails(screw-in type)

The soil nail(s) were carefully pushed or screwed into the slope mid-height based on the predetermined configurations. After each test, the deformation and collapse underwent by the slope were measured and captured on photographs for further analysis.

3. RESULT ANALYSIS AND DISCUSSIONS

3.1 Proof of concept: Improved shear resistance
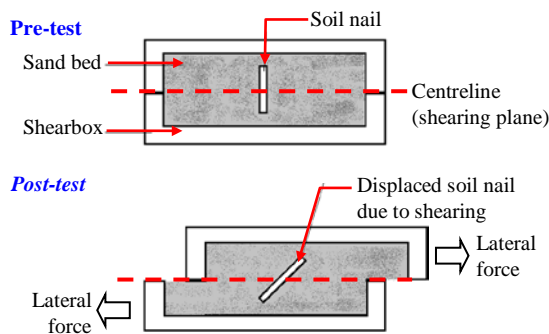
Fig. 6 Setup of the shearbox test.
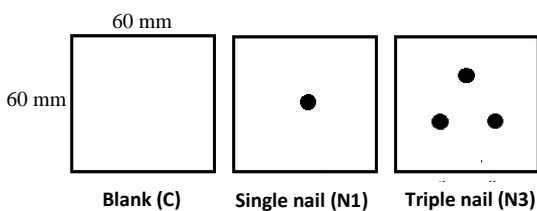
Fig. 7 Configurations in shearbox with and without nail installation.
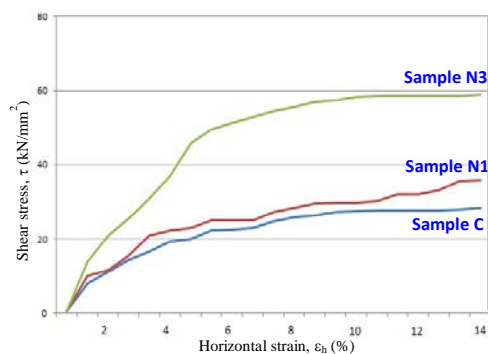
Fig. 8 Shear stress (τ) vs. horizontal strain (ε_h) plots for the shearbox tests.

In order to determine the correlation between number of nails installed and the resulting shear resistance, a series of shearbox tests was carried out (Fig. 6). Laying a layer of loose sand as the soil bed ($\rho = 1.6$ g/cm^3), ordinary 1.2 cm long screws were next installed as representative soil nails. Excluding the control 'blank' sample, 2 other samples tested included the single and triple nail configurations (Fig. 7). All samples were subjected to the same small vertical stress of 0.83 N/cm^2.hearing of the sample took place with two equal halves of the shearbox sliding horizontally in opposite directions (Fig. 6). The shearing plane was fixed as the horizontal plane at mid-height of the sample.

From the tests, it was shown that the nail(s) installation could effectively increase overall shear resistance. As depicted in Fig. 8, the control sample (C) recorded the lowest peak shear stress (τ), while the samples with nail installation, especially N3 showed significant shear resistance improvement, i.e. twice that of the soil's original shear strength (see Sample C). The single nail installation (N1), on the other hand, contributed marginally to shear resistance enhancement.

It is worth noting that in this test series where other configurations were explored, besides the number of nails per unit area, the arrangement of nails appeared to influence the development of shear resistance too. Installation of 3 nails in a single row, for instance, could have a different shear resistance evolution pattern compared to 3 nails in a triangular formation. However these are beyond the scope of the present paper and are not included in the discussions.

3.2 Angular Distortion Ratio (θ_R)
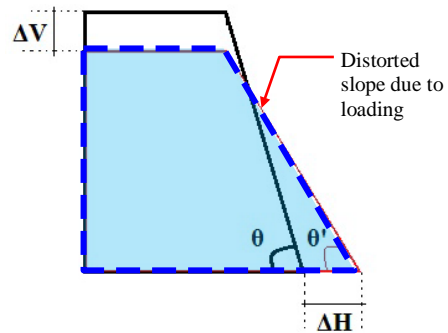
Fig. 9 Angular distortion of slope: θ = pre-failure, θ' = post-failure.

In the model tests, under the constant loading of 700 kPa, the slopes, reinforced or not, underwent deformation and distortion to various degrees. Part of the slope crest also showed signs of collapse in the overall movement of the slope with increased stress application.

In order to gauge the severity of the slope's distortion, the Angular Distortion Ratio (θ_R) was defined based on the changes of the slope's inclination angle before and after failure (Fig. 9). The vertical and horizontal displacements are denoted by ΔV and ΔH respectively. The resulting slope angles pre- and post-failure were then derived using simple trigonometry as follows:

- Original slope angle, $\theta = \tan^{-1}(V/H) = 70.35°$
- Post-failure slope angle, $\theta' = \tan^{-1}(V'/H')$
- Angular change, $\Delta\theta = \theta - \theta'$
- Angular Distortion Ratio, $\theta_R = \Delta\theta/\theta$

Table 1. Slope distortion parameters post-test.

Sample	Settlement, ΔV (cm)	Horizontal displacement, ΔH (cm)	Post-failure slope angle,θ'(°)	θ_R
C	5	14	43.78	0.38
CN1	5	12	46.27	0.34
CN3	5	9	50.44	0.28
IN1	5	9	50.44	0.28
IN3	4	8	53.13	0.24

Table 1 summarizes the displacement parameters (i.e. ΔV, ΔH and θ') and the calculated θ_R for all simulated slopes in the model tests. Note that all tests were terminated at failure settlements no more than the preset 20 %, i.e. ΔV ranged between 15 to 18 % from the original height of 28 cm. Settlement of the slope crest is mainly attributed to the compression of the loosely compacted backfilled SKW. On the other hand, the efficacy of soil nails can only take effect when a threshold shear strength of the reinforced composite is mobilized [10]. It would seem that at 700 kPa, approximately 5 cm settlement of the crest was necessary to both initiate actual loading of the slope with compression of the relatively loose soil, and to mobilize shear resistance of the reinforced slope (excluding sample C).It is not possible though at present to differentiate the compression of the soil and the minimum displacement required for shear resistance mobilization. Hence, the slope's distortion was derived from the horizontal displacement (ΔH), which measured 27 to 47 % of the original base width, 30 cm. This resulted in the distortion of the slope as recorded in the post-failure slope angle, θ' (Fig. 9).

As expected, sample C (control) suffered the most severe distortion without any reinforcement. When a single control nail was installed (CN1), θ_R dropped by 11 %, clearly indicating the efficacy of the soil nail in shear resistance enhancement. With 3 control nails in place (CN3), θ_R underwent further reduction, i.e. 26 %, which is about 1.2 times lower than that of CN1. With the screw-in nails, the single nail sample (IN1) produced the same θ_R as CN3, i.e. 0.28, suggesting the same shear resistance mobilized. In other words, a single screw-in nail is equivalent to 3 conventional smooth surface nail in terms of shear resistance. The most effective counter-distortion was observed in sample IN3, where the triple screw-in nail

configuration gave the lowest θ_R of 0.24.

The Angular Distortion Ratio (θ_R) analysis also indicates the nature of slope movement. The slope failure mechanism as simulated in the model tests points to the shallow landslide type failure, involving large volume of sliding mass from multiple rupture planes in the slope's mass (Fig. 10). The ruptures may trigger both rotational and translational failures along the slope. In order to quantify the volume displacement of the slope failures observed in the tests, the Volumetric Deformation Index (V_D) was next derived.

3.3 Volumetric Deformation Index (V_D)

As the slope approached failure, shallow rotational as well as translational mechanisms were initiated simultaneously, resulting in partial collapse of the slope. This is illustrated in 2-dimensional form in Fig. 10, where each square grid is 5 cm x 5 cm. The weakened slope body underwent gradual displacement which eventually led to disengagement along the multiple rupture plane, i.e. collapsed zone. The dislodged soil mass then rolled down the slope and formed a heap at the foot of the slope, i.e. residual zone. Taking the principle of mass conservation, the ruptured and dislodged soil mass near the top of the slope must equal the soil heap found at foot of the slope. In other words, the 2D image captured in Fig. 10 should demonstrate that unit area of the collapsed zone equates unit area of the residual zone.

It is however noticeable in Fig. 10 that this is not the case. For instance, the unit area of the 2 zones in the control sample (C) were incompatible, where the collapsed zone showed an excess of 1 square unit. Indeed, the unit area for the collapsed zone is consistently in excess of the residual zone for all cases, suggesting volume loss in the original slope not caused by rupture-related soil mass dislodgement. This could account for the compression of the soil under loading mentioned in 3.2, where the overall density of the slope mass was to a certain extent increased by the applied load. Notwithstanding this insight, the threshold deformation required to mobilize the shear resistance remains undefinable.

Table 2 shows the volumetric change parameters and the calculation of V_D. Assuming that the failure pattern captured on the square grids to be uniform throughout the length of the slope, the slope's volumetric deformation can be estimated from the unit area itself. Therefore, multiplication of the total unit area of collapsed zone with the depth of the model box (30 cm) gives the corresponding volumetric deformation (ΔV). The Volumetric Deformation Index (V_D) is next derived simply by dividing ΔV with the original slope's volume.

Referring to Table 2, the single nail

installation, i.e. CN1 and IN1, improved the volumetric deformation only marginally compared to that of the unreinforced slope (control sample, C). With the triple nail configuration, both nail types exhibited significant control and reduction of volume change in the slope, where CN3 and IN3 recorded 24 and 33 % reduction in V_D respectively relative to sample C.
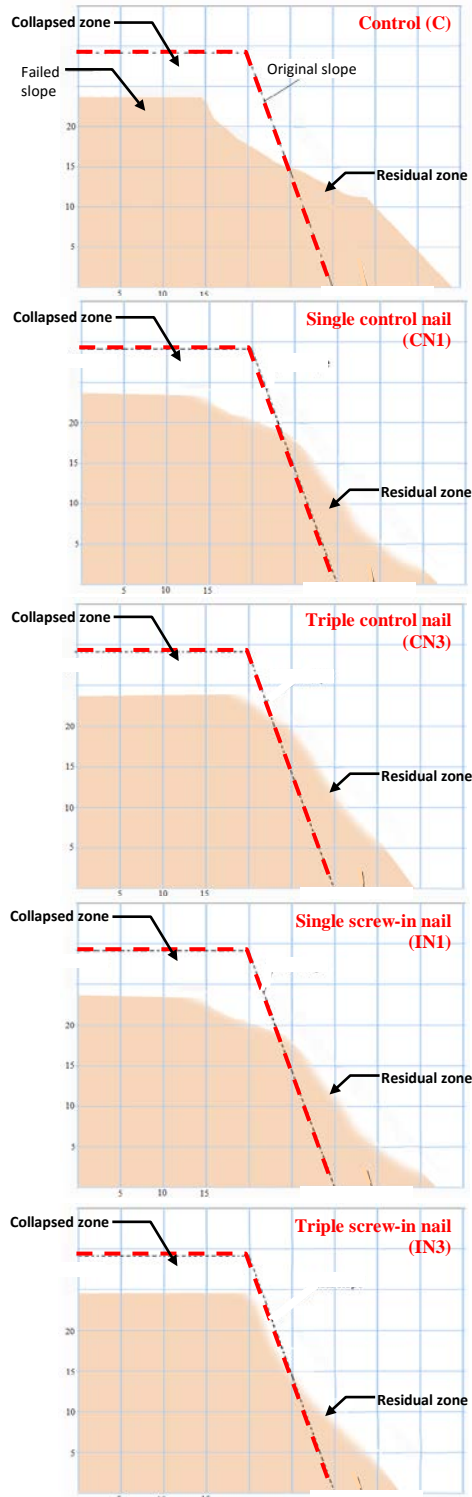
Table 2. Volumetric change assessment.

Sample	Area of collapsed zone (cm^2)	Volumetric deformation, ΔV (cm^3)	Volumetric Deformation Ratio, V_D
C	150	4500	0.21
CN1	137.5	4125	0.20
CN3	112.5	3375	0.16
IN1	137.5	4125	0.20
IN3	100	3000	0.14

The effectiveness of the screw-in soil nail in stabilizing the slope is evident in the post-failure graphical representation of Fig. 10. Note that only the slope's volumetric displacement was examined in conjunction with the stabilization measures incorporated, where any progressive localized straining were not taken into consideration due to the relatively small scale model setup. In corroboration with the V_D values obtained (Table 2), the single nail installation for both CN1 and IN1 resulted in very similar failure pattern: significant crest subsidence and near-crest rupture, though the residual zone area indicates about 30 % less soil heap in both cases compared to the control. With the triple nail installation, CN3 clearly suffered less near-crest collapse with less spreading of the dislodged material at the foot of the slope. In comparison, IN3 showed nearly zero near-crest rupture with top half of the slope remained almost intact, where the dislodged material seemed to be traced from the bottom half of the slope. It follows that the relatively small residual zone observed in IN3 was the result of material dislodged from the unreinforced bottom half of the slope.

These failure patterns shed light on the shear resistance enhancement of the screw-in soil nail. Apparently the nails provide better reinforcement than the conventional nails. This could be due to several key factors:

a. The screw-in installation technique created less disturbance to the soil, hence leaving the soil's shear strength mostly unchanged.
b. The helical spiral surface and hollow stem gave better soil-nail grip with larger contact surface and better interlocking.
c. The nails enabled more effective load transfer and distribution mechanism within the slope mass to prevent propagation of the rupture planes.

4. CONCLUSIONS

A model simulation of slope reinforced with soil nail(s) was conducted with conventional smooth surface nails as well as the innovative screw-in type nails. The tests showed up to 37 % angular distortion reduction and 33 % improvement in terms of volume deformation. The

Fig. 10 Graphical representation of post-failure slopes as captured in the model tests.

indices derived, θ_R and V_D suggest overall enhanced shear resistance of the slope against excessive movements, particularly the shallow landslide type failures. Further work could be extended to ascertain more varied aspects of in situ conditions, such as groundwater fluctuation, slope inclination, loading as well as the soil's intact shear strength.

5. ACKNOWLEDGEMENT

6. REFERENCES

[1] Greenfield, S. J. (1992). Foundation in Problem Soils. Englewood Cliffs. N.J.: Prentice-Hall.

[2] Cai, J. & Ugui, K. (2004). Numerical analysis of rainfall effects on slope stability. International J. of Geomechanics, vol. 4, issue 2, 69-78.

[3] Dahal, R., Hasegawa, S., Tamanaka, M., Dhakal, S., Bhandary, N. & Yatabe, R. (2009). Comparative analysis of contributing parameters for rainfall-triggered landslides in the Lesser Himalaya of Nepal. Environmental Geology, vol. 58. no. 3, 567-586.

[4] Deepa, V. & Viswanadham, V. S. (2009). Centrifuge model tests on soil-nailed slopes subjected to seepage. Ground Improvement, vol. 162, issue 3, 133-144.

[5] Guan, J., Mok, C. & Yeung, A. (2014). Integrated analysis framework for predicting surface runoff, infiltration and slope stability. Geo-Congress 2014, 2588-2599.

[6] Raj, M. & Sengupta, A. (2014). Rain-triggered slope failure of the railway embankment at Malda, India. Acta Geotechnica, vol. 9, no. 5, 789-798.

[7] Abramson. (2001). General Slope Stability Concepts.P1: UFA PB051-01

[8] Ali, M. F. (2014). Erosion assessment of slope failure tragedies; Case study in Malaysia. Applied Mechanics and Materials,vol. 567, pg.711-716.

[9] Morgan, R. P. C. Soil Erosion and Conservation, 3rd ed. (2009).UK: John Wiley & Sons, Ltd.

[10] Prashant, A. & Mukherjee, M. (2010). Soil Nailing for Stabilization of Steep Slopes near Railway Tracks. Department of Civil Engineering, Indian Institute of Technology Kanpur.

[11] www.china-steelpiling.com (accessed 24 April 2016).

[12] Federal Highway Administration. (2015). FHWA Manual FHWA-NHI-14-007: Geotechnical Engineering Circular No. 7- Soil Nail Walls. USA: FHWA.

[13] British Standards Institution. (2011). BS8006-2: 2011 Code of Practice for Strengthened / Reinforced Soils- Part 2: Soil Nail Design. UK: BSI.

[14] British Standards Institution. (2010). BS EN 14490: 2010 Execution of Special Geotechnical Works: Soil Nailing. UK: BSI.

[15] Xiao, M. (2015). Geotechnical Engineering Design. UK: John Wiley & Sons, Ltd.

[16] Mcdonald, P. & Ims, B. (2006). Soil-nailed retention- A practical approach to field verification. Australian Geomechanics, vol. 41, no. 3, 93-99.

[17] Su, L., Chan, T., Yin, J., Shiu, Y. & Chiu, S. (2008). Influence of overburden pressure on soil-nail pullout resistance in a compacted fill. J. of Geotechnical & Geoenvironmental Engineering, vol. 134, issue 9, 1339-1347.

[18] Pei, H., Yin, J., Zhu, H. & Hong, C. (2013). Performance monitoring of a glass fibre-reinforced polymer bar nail during laboratory pullout test using FBG sensing technology. Int. J. of Geomechanics, vol. 13, issue 4, 467-472.

[19] Wang, Z. & Richwien, W. (2002). A study of soil-reinforcement interface friction. J. of Geotechnical & Geoenvironmental Engineering, vol. 128, issue 1, 92-94.

[20] Yin, J-H., Su, L-J., Cheung, R. W. M., Shiu, Y-K. & Tang, C. (2009). The influence of grouting pressure on the pullout resistance of soil nails in compacted completely decomposed granite fill. Geotechnique, vol. 59, issue 2, 103-113.

[21] Yin, Y. & Xu, Y-L. (2015). Design on soil-nailing wall supporting of foundation pit in Bao Tou. Proc. 5th Int. Conf. on Advanced Design & Manufacturing Engineering (ICADME2015), 19-20 Sep 2015, Shenzhen, China.

[22] Turner, J. & Jensen, W. (2005). Landslide stabilization using soil nail and mechanically stabilized earth walls: Case study. J. of Geotechnical & Geoenvironmental Engineering, vol. 131, issue 2, 141-150.

[23] Li, X. (2007). Finite element analysis of slope stability using a nonlinear failure criterion. Computers & Geotechnics, vol. 34, 127-136.

[24] Farshidfar, N. & Nayeri, A. (2015). Slope stability analysis by shear strength reduction method. J. of Civil Engineering & Urbanism, vol. 5, issue 1, 35-37.